Section 8

Development of and advances in ocean, sea-ice, and wave modelling and data assimilation.

Infrasound radiation from sea waves: Sensitivity to climate changes

I.P. Chunchuzov[1] and I.I. Mokhov[1,2]

[1]A.M. Obukhov Institute of Atmospheric Physics RAS

[2]Lomonosov Moscow State University

igor.chunchuzov@gmail.com

mokhov@ifaran.ru

It is interesting to estimate possible variations of infrasound activity (intensity of microbaroms and "voice of the sea") associated with variations of temperature, wind and intensity of sea waves under climate changes. The source strength spectral density for infrasound radiation from sea waves to the atmosphere was obtained in [1] and can be presented in the following form

$$\mathrm{S}(f) = \frac{4\pi^4 \rho_{air}{}^2 g^2 f^3}{c_{air}{}^2}\left[\frac{c_{air}{}^2}{c_w{}^2} + \frac{9g^2}{4\pi^2 c_{air}{}^2 f^2}\right] W(f) \qquad (1)$$

where $W(f) \equiv \int_0^{2\pi} F(f/2,\theta) F(f/2,\theta+\pi)\,\mathrm{d}\theta$ is the so-called Hasselmann term, which is an integral over all directions of the product of frequency-angular spectra of sea waves $F(f/2,\theta)$ taken in opposite directions [1], c_{air} is the sound speed in the atmosphere, ρ_{air} is the atmospheric density, c_w is the sound speed in the water, g is the gravity acceleration and f is the frequency. If infrasound sources are uniformly distributed within a certain area A of the ocean, then at a distance R that is much larger than the size of this area, the spectral density of infrasonic pressure pulsations $<\left|\hat{P}(R,f)\right|^2>$ is equal to the product $A \cdot S(f) \cdot Q(R,f)$, where $Q(R,f)$ is the transfer function of the atmosphere through which the infrasound propagates from the region of its radiation to the point of observation. The term $W(f)$ takes non-zero values only in case of existence of nonlinear interactions between counter propagating surface waves. Such conditions arise in case of occurrence of a strong atmospheric vortex over the ocean surface so that the wind vector turns and becomes opposite to the background wind field. At typical values of the sound speed in air and water and the maximum of the microbarom spectrum at $f \approx 0.2$ Hz , the ratio of the second term in the square brackets in (1) to the first one is about 0.08. The main contribution to infrasound radiation (1) into the atmosphere is caused by pressure fluctuations in the water generated by water-air interface motions:

$$S(f) = \left[\frac{4\pi^4 \rho_{air} g^2 f^3}{c_w{}^2} + \frac{4\pi^4 \rho_{air} g^2 f^3}{c_{air}{}^4}\left(\frac{9g^2}{4\pi^2 f^2}\right)\right] W(f,u^*) = \frac{4\pi^4 \rho_{air} g^2 f^3}{c_w{}^2}[1+\eta] W(f,u^*) \qquad (2)$$

$$\eta = \frac{9g^2}{4\pi^2 f^2}\frac{c_w{}^2}{c_{air}{}^4} << 1$$

It is taken into account in (2) that the sea wave spectrum depends on the dynamic friction velocity u^*, the sound speed in water c_w and in air c_{air} . The relative changes in the infrasound source strength spectrum at a fixed frequency can be approximately presented as

$$\frac{dS}{S} = -\left(\frac{2dc_w}{c_w} + \frac{4\eta dc_{air}}{c_{air}}\right) + \frac{\partial W}{\partial u^*}\frac{du^*}{W} \qquad (3)$$

There are different models of the sea-wave spectrum [2]. For example, the models both by Kitaygorodsky and Zakharov lead to the following spectrum of the surface vertical displacements

h [2]: $F_h(f) = \alpha u* g\omega^{-4}$, where α is a numerical constant. Since W is proportional to the product of the sea surface spectra and therefore to $u*^2$, the last term in (3) becomes $2du*/u*$. It characterizes the relative changes in the wind vertical shear within the atmospheric vortex over the ocean surface.

It can be shown that the relative changes in the speed of sound in water and air (the first two terms in (3)) arising because of the increase in air and water temperatures by 1 deg are two orders of magnitude less than the contribution to source strength spectrum (3) due to wind shear changes (the last term in (3)) as large as 1 m/s per 20 m. Thus, the problem of finding relative changes in source strength of infrasound radiation is associated with relative changes in the sea wave interaction integral *W*. In [3] the infrasound source strength during stratospheric warmings was predicted by using the 2D wave energy spectrum obtained from the ECMWF ocean wave model.

Microbarom observations at a network of infrasound stations around the globe do reveal an increase in the intensity of the microbarom radiation when the wind speed increases in tropical cyclones [1]. However, at large distances (hundreds and thousands of km) from the ocean area occupied by storm winds, the changes in the infrasound source strength are masked by the influence of the stratospheric stratification on the microbarom amplitudes. The sensitivity and contributions of various terms in (3) can be estimated from climate model simulations with different scenarios of natural and anthropogenic forcings [4].

This work has been supported by the Russian Science Foundation (project No. 19-17- 00240) using the results obtained in the framework of the RAS Presidium program "Climate change: causes, risks, consequences, problems of adaptation and regulation" and by RFBR (No No 18-55-05002, 17-05-01097).

References

1.Waxler R. et al., Generation of microbaroms by deep-ocean hurricanes / In: Infrasound Monitoring for Atmospheric Studies. Ed. by A. Le Pichon, E. Blanc, A. Hauchecorne. Springer. 2010, 735 pp.

2.Golitsyn G.S. Methodical foundations of the theory of turbulence and sea waves. Izv. Atmos. Oceanic Phys., 2001, **37** (4), 406-413.

3.J.D.Assink, R.Waxler, P.Smets,and L.G.Evers. Bidirectional infrasonic ducts associated with sudden stratospheric warming events. J. Geophys. Res. Atmos., 2014, 119, doi:10.1002/2013JD021062.

4.Khon V.C., Mokhov, I.I., Pogarskii F.A. Estimating changes of wind-wave activity in the Arctic ocean in the 21st century using the regional climate model. Doklady Earth Sci., 2013, **452** (2), 1027-1029.

Data Assimilation for the Real Time Ocean Forecast System

Zulema D. Garraffo[1], James A Cummings[1], Ilya Rivin[1], Shastri Paturi[1], Yan Hao[1], Todd Spindler[1], Avichal Mehra[2]
(1)IMSG at NOAA/NWS/NCEP/EMC, College Park, MD, USA; (2)NOAA/NWS/NCEP/EMC, College Park MD, USA.
Email: zulema.garraffo@noaa.gov; phone: 301-683-3744

Introduction

Global high resolution data assimilation simulations were produced as a step towards building the RTOFS-DA (Real Time Ocean Forecast System with Data Assimilation). RTOFS-DA is based on the Navy Coupled Ocean Data Assimilation (NCODA) system (Cummings and Smedstad, 2013). The current operational RTOFS, version 1.1.4, produces forecasts starting from daily analyses provided by the HYCOM based Global Ocean Forecast System, version 3.1, operational at the U.S. Naval Oceanographic Office (Metzger et al., 2014). Instead, analyses will be produced through RTOFS-DA when in operations. RTOFS and RTOFS-DA use the HYbrid Coordinates Ocean Model (HYCOM, Bleck 2002) at 1/12° resolution and 41 vertical hybrid layers coupled with Los Alamos Community Ice CodE (CICE).

Simulations

We present results from simulations with 2017 historical data, and discuss the setup for a near real time simulation being started in 2019. All simulations are performed on the tri-polar global 1/12° horizontal resolution domain with 41 vertical hybrid layers, and are forced with atmospheric analysis fields from the NOAA/NCEP Global Data Assimilation System (GDAS).

Externally produced quality controlled data are used for the 2017 simulations. The observational data consist of the following: sea surface height (SSH) from the CryoSat, Jason, Sentinel, Altika altimeters; sea surface temperature (SST) retrievals from NOAA (18, 19), and METOP (A, B); surface temperature from in-situ measurements (fixed and drifting buoys, ships); subsurface profiles of temperature and salinity from Argo, XBT, CTD, and glider data; and sea ice coverage from SSMI/S and AMSR2. With the exception of SSH, all data are obtained from the Global Ocean Data Assimilation Experiment (GODAE) server. SSH observations are obtained directly from the Altimeter Processing System (ALPS) at the Naval Oceanographic Office.

The 3D-VAR analysis is performed using a 24-hour update cycle with the analysis time centered on the update cycle interval. The observations are pre-processed as follows; SST observations are averaged to form super-observations to remove data redundancies using local correlation length scales; background error variances are computed from a 15-day history of forecast differences using forecasts separated by a 48-hour time interval (twice the analysis update cycle). The 3D-VAR analysis is performed directly on the HYCOM global horizontal grid, and uses hybrid vertical coordinates valid at the analysis time. The global ice coverage analysis is incorporated through the CICE model. The 3D-VAR analysis increments for temperature, salinity, velocity, and layer thickness are incorporated into the forecast model using an incremental analysis update procedure where the corrections are inserted into the ocean model starting 3 hours earlier than the analysis time. The forecast is then issued from this balanced initial state.

For a first historical simulation covering one year, February 2017-January 2018, altimeter SSH is incorporated using bi-monthly climatological relationships between SSH (dynamic height) and temperature and salinity at depth in the form of synthetic temperature and salinity profiles (MODAS, Fox et al., 2002). MODAS assimilates SSH anomalies (SSHA) from a long term mean. A strong limitation with using MODAS is that the synthetic profiles do not incorporate any information from the forecast model. In addition, a shorter simulation covering the period October-December 2017 was performed by assimilating altimetry SSH observations in the form of Absolute Dynamic Topography (ADT). Here, the ADT measurements are referenced to the model forecast SSH. The observed difference is then used to directly adjust the HYCOM temperature, salinity, and layer structure so the model forecast SSH now matches the altimeter ADT. A modified version of the Cooper and Haines (1996) method is used. The modifications include constraining the solution with updated estimates of SST, SSS, and model mixed layer depth. Work continues to improve the method by developing multivariate constraints between the ADT innovations and the barotropic stream function in HYCOM, which should improve the use of altimeter data in mid to high latitudes.

Results

For the long-term simulation with MODAS profiles, the total temperature verification averaged across the grid results in very small biases (not shown) during the length of the simulation. A few days after initialization, the global total temperature verification RMS error reaches a stable value of 0.5°C, with a slight increase during the Northern Hemisphere summer. The Argo temperature verification RMS error is 0.8°C, with a seasonal cycle similar to that of the total RMS temperature. The Argo temperature mean bias is 0.1°C.

Vertical sections for verification of total, Argo and MODAS temperature show very small residuals (Observations minus Analysis, Figs. 1a, b, c lower panel, respectively), implying that the observations are effectively analyzed. The section for total temperature bias for innovations (Observations minus 24-hour Forecast) shown in the Fig. 1a upper panel closely follows the MODAS bias (Fig. 1c upper panel). The model 24-hour forecasts of Argo temperature are consistently cold-biased below 100m, and are relatively unbiased near the surface due to the simultaneous assimilation of

satellite SST (Fig. 1b upper panel). The similarity of the total and MODAS biases indicates that the lack of skill in forecasting Argo temperature at depth is likely due to the assimilation of MODAS synthetics.

A 3-month (Oct-Dec, 2017) simulation employing assimilation of ADT altimetry shows improved subsurface temperature forecast of Argo profiles. HYCOM forecasts the ADT observations very well with SSH innovations on the order of 10 cm or less away from western boundary currents, where model corrections can be large due to errors in the positions of ocean fronts. There is a consistent ~0.5 m difference between the HYCOM and ADT SSH across all satellite altimeters and ocean basins that is easily corrected. ADT observations are more accurate because the data incorporate geoid information instead of a model-based reference mean dynamic topography. Whole ocean averages of total temperature and Argo temperature RMS error for the ADT simulation result in similar values compared to the MODAS simulation (0.5°C and 0.8°C respectively).

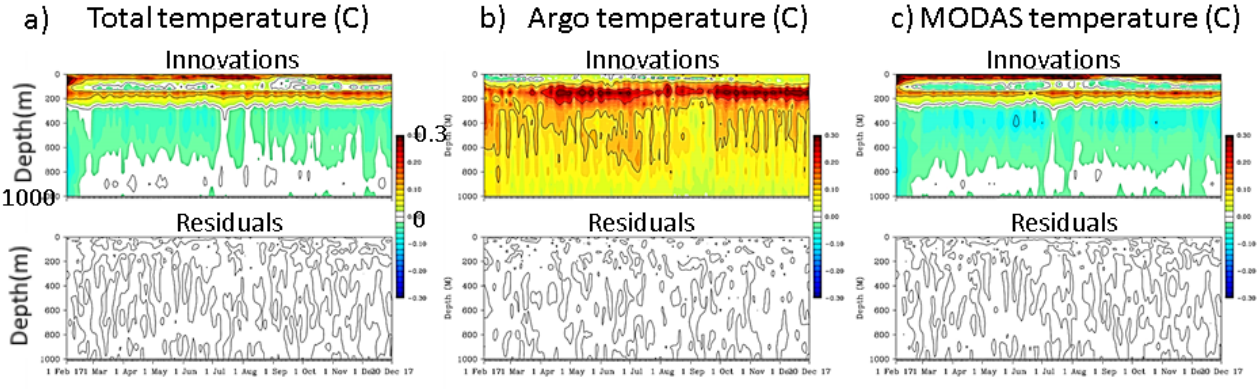

Figure 1. MODAS simulation, temperature bias verification for vertical sections, horizontal global averages at each depth vs. time, in the upper 1000 m, Feb-Dec 2017 (°C) : a) Total temperature innovations (observations – forecast, top), and residuals (observations – analysis, bottom); b) same as a) but for Argo Float temperature; c) same as a) but for MODAS temperature.

For the two simulations, the global SSH field for the ADT simulation shows less large scale drift from its verified initial condition. For these reasons, assimilation of the ADT observations using the direct corrections to the HYCOM layer structure is currently selected as the best approach.

The temperature bias verification in vertical sections for the ADT simulation (Oct-Dec 2017) are shown in Fig. 2a, b. The innovation bias for total temperature closely follows the Argo temperature bias, with a maximum bias of about 0.5°C at a depth of about 170m. Tests are underway to reduce this bias. The global SSH towards the end of the simulation (Dec 8 2017, Fig. 2c) shows an active eddy field. No large scale drift is noted during the 3 months of the simulation.

A real-time setup based on the ADT simulation is planned for operational implementation at NCEP.

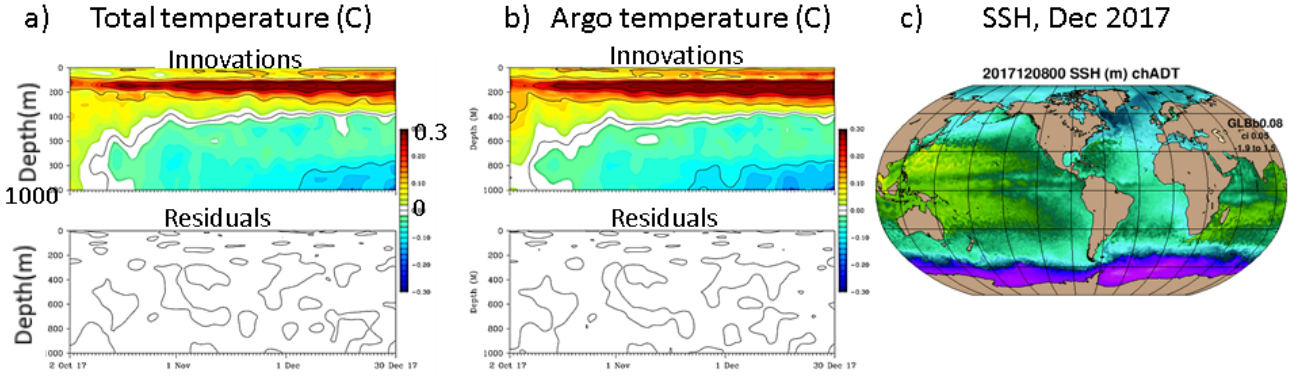

Figure 2. ADT simulation, October-December 2017: a) Temperature bias verification vertical sections: total temperature innovations (observations – forecast, top, °C), and residuals (observations – analysis, bottom); b) same as a) but for Argo Float temperature; c) SSH (m), 2.5 month from the beginning of the simulation.

References

Bleck, R. 2002. An oceanic general circulation model framed in hybrid isopycnic-Cartesian coordinates, *Ocean Model.*, 4, 55-88.

Cooper M, Haines KA, 1996. Altimetric assimilation with water property conservation. J. Geophys Res 24, 1059-1077

Cummings, J. A. and O. M. Smedstad. 2013. Variational Data Assimilation for the Global Ocean. Data Assimilation for Atmospheric, Oceanic and Hydrologic Applications (Vol II) S. Park and L. Xu (eds), Springer, Chapter 13, 303-343.

Fox, D.N, C.N. Barron, M.R. Carnes, M. Booda, G. Peggion, J.V.Gurley, 2002.The Modular Ocean Data Assimilation System. Oceanography 15 (1): 22-28

Mehra, A.; I. Rivin; Z. Garraffo; B. Rajan, 2015. Upgrade of the Operational Global Real Time Ocean Forecast System, 2015. In: Research Activities in Atmospheric and Oceanic modeling, Ed. E.Astakhova, WMO/World Climate Research Program Report No.12/2015. http://bluebook.meteoinfo.ru/uploads/2015/chapters/BB_15_s8.pdf

Metzger, E.J; O.M. Smedstad; P.G. Thoppil; H.E. Hurlburt; J.A. Cummings; A.J. Wallcraft; L. Zamudio; D.S. Franklin; P.G. Posey; M.W. Phelps; P.J. Hogan; F.L. Bub; and C.J. DeHaan, 2014. US Navy Operational Global Ocean and Arctic Ice Prediction Systems. *Oceanography* 27(3):32–43 http://dx.doi.org/10.5670/oceanog.2014.66

NCEP HWRF-HYCOM-WW3 Forecast System

Hyun-Sook Kim[1,2], Jessica Meixner[2], Alan Wallcraft[3], Dmitry Sheinin[1,2], Avichal Mehra[2], Vijay Tallapragada[2]
[1]IMSG at EMC/NCEP/NWS/NOAA, College Park, MD 20740; [2]EMC/NCEP/NWS/NOAA, College Park, MD 20740;
[3]COAPS of FSU, Tallahassee, FL 32306
Email: Hyun.Sook.Kim@noaa.gov

1. Introduction

Development of a 3-way coupling HWRF-HYCOM-WW3 modeling system has been completed at EMC/NCEP/NWS/NOAA. This new system (Fig. 1) adds WW3 (WAVEWATCHIII) to the existing 2-way coupled HWRF-HYCOM system (Kim et al. 2014), to better represent complex air-sea interaction processes. Interactions with the wave model in the system include: i) generation of lengths that depend on wave age, which in turn modify drag coefficients and wind stress; and, ii) the capability to simulate wave-current interactions and enhance KPP turbulent mixing with instabilities associated with these interactions (Langmuir mixing). HYCOM receives wave-induced Coriolis-Stokes forcing in the form of Stokes drift that later interacts with oceanic currents at upper ocean depths, and HYCOM generates a Langmuir number based on Langmuir mixing. The specific role of the Langmuir number (La) in HYCOM is to modify turbulent velocity scales. HYCOM v3 has four options for calculating La (see Table 1) based on suggestions published by McWilliams and Sullivan (2001), Smyth et al. (2002), Harcourt and D'Asaro (2008), and Takaya et al. (2010).

The 3-way coupled system uses a default setting wherein at each coupling step WW3 sends a set of surface mean Stokes drift (*Us,Vs*) and wave-number (k) averaged over total 25 wave lengths to HYCOM. In turn, HYCOM projects these mean values to sub-surface depths, using an exponential function (e^{kz}) where z represents ocean depths.

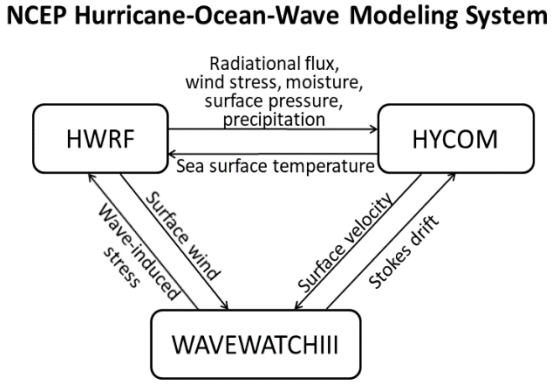

Figure 1. Schematic representation of NCEP 3-way coupled modeling system.

Table 1. List of experiments:

#	Reference
HW31	McWilliams and Sullivans (2001). Spill Sci. Tech. Bull., 6
HW32	Smyth et al. (2002). Ocean Dynamics, 52
HW33	McWilliams and Sullivans (2001). Spill Sci Technology Bull., 6; Harcourt and D'Asaro (2008). J. Phys. Oceanogr.,38
HW34	Takaya et al (2010), J. Geophys. Res., 115
HW35	Takaya et al (2010), J. Geophys. Res., 115; and Breivik et al. (2014); $k=k_m/3$ (k_m=mean surface wavenumber)

2. Model configurations

HWRF is a triply-nested domain, solving a Non-hydrostatic Mesoscale Model (NMM) dynamic core in the earth-rotated Arakawa E-staggered grid at a horizontal resolution of 1.5/4.5/13/5-km and 75 hybrid-pressure-sigma levels. The set of physics, radiation effects, vertical diffusion and the land surface model employed are discussed in more detail in https://dtcenter.org/HurrWRF/users/docs/users_guide/HWRF_v3.7a_UG.pdf. Initial and boundary conditions (ICs/BCs) are provided from the grib2 products of the EMC new global model FV3GFS (v15). As part

of the initialization, HWRF uses data assimilation based on GSI (Gridpoint Statistical Interpolation) hybrid ensemble 3D-Var data assimilation (DA). HYCOM solves 3D free-surface, primitive equations on a staggered Arakawa C-grid at a resolution of 1/12-degree and 41 pressure-z hybrid levels. Sub-grid physics are represented by the KPP mixing scheme. ICs and BCs for HYCOM are a subset of the Global Real-Time Operational Forecast System. WW3 is a spectrum model that simulates surface waves at a resolution of 25 in frequency from 1.1 Hz and 24 in the direction from true north. BCs for the solution are obtained from previous cycle's global wave multi_1 run, while ICs utilize a restart file from current cycle's global wave multi_1 run.

We have performed sensitivity experiments for different La options (as shown in Table 1), including an experiment with a reduction in wavenumber by a factor of 3 (e.g., Breivik et al. 2014). The experiments focus on Hurricane Michael (14L) from 2018 in the North Atlantic basin. Each experiment produces 22 cycles of 5.25-day simulations in total, to cover the entire lifecycle of the storm. Except for the first cycle, each model component, except WW3, uses a warm start using 6-hour coupled forecasts from the previous cycle. When Tail Doppler Radar observations are available, HWRF initialization also uses a hybrid self-cycled DA method based on a 40-member HWRF ensemble, in place of the GSI ensemble. This self-cycled DA was performed for a total of 6 cycles that extend from October 7 12Z to October 8 18Z. This paper presents an introduction to the 3-way coupling forecast system, and briefly reports on preliminary results of this sensitivity study.

3. Results and discussion

Fig. 2 shows comparisons of verified track and intensity forecasts for the five experiments, also including 2-way coupling runs with the 2018 operational HWRF (forced by GSMGFS; HWRF in Fig. 2), FV3GFS forced HWRF-POM (S219) and HWRF-HYCOM (Y219). For track forecasts, HW34 and HW35 show the smallest errors for all lead times, and Y219 simulates the worst track (Fig. 2A). The worst intensity forecast is found with S219, having the maximum AME of 32.6 kt at 66-hr forecast (Fig. 2B). It appears that HW33 predicts smallest intensity error, and all the 3-way coupled runs improve on the AME from the 2-way coupled experiment. As for intensity bias (Fig. 2C-2D), all simulations have a negative bias. However, S219 shows the worst forecast, having the largest negative bias for Vmax and the largest positive bias for Pmin. The second worst run is with Y219. Different representations of Langmuir mixing result in different Vmax bias errors as large as O(10 kt). However, their bias for Pmin is either positive for the HW32 setup or negative for the HW33 configuration. The rest of the experiments vary in between these two.

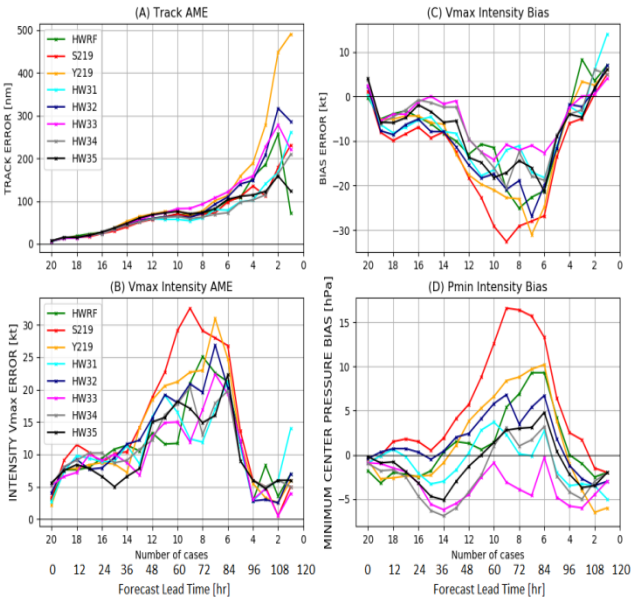

Figure 2. Absolute mean error (A-B), and bias (C-D) comparisons: HWRF is the 2018 operational coupled HWRF-POM (Princeton Ocean Model) forced by GSM (Global Spectrum Model)GFS, S219 is HWRF-POM forced by FV3GFS, and Y219 is HWRF-HYCOM forced by FV3GFS.

Preliminary results suggest that the 3-way coupling evidently improves both track and intensity forecasts over 2-way coupling. However, a more extensive analysis with a larger sample of storms is required to reach a robust conclusion. Overall, it is encouraging that an adjustment of the 3-way coupling system can improve hurricane forecasts.